STEM CELLS®

EMBRYONIC STEM CELLS/INDUCED PLURIPOTENT STEM CELLS

CHD2 is Required for Embryonic Neurogenesis in the Developing Cerebral Cortex

TIANJIN SHEN[1,2,#], FEN JI[1,#], ZENGQIANG YUAN[3], AND JIANWEI JIAO[1,*]

[1]State Key Laboratory of Reproductive Biology, Institute of Zoology, Chinese Academy of Sciences, Beijing 100101, China; [2]University of Chinese Academy of Sciences, Beijing 100049, China. [3]State Key Laboratory of Brain and Cognitive Sciences, Institute of Biophysics, Chinese Academy of Sciences, Beijing 100101, China.

*To whom the correspondence should be addressed: Jianwei Jiao, Ph.D, Principal Investigator, Group of Neural Stem Cell and Neurogenesis, Institute of Zoology, Chinese Academy of Sciences, 1 Beichen West Road, Chaoyang District, Beijing 100101, P.R.China, Tel: 86-10-64806335; Email: jwjiao@ioz.ac.cn; [#]These authors contributed equally to this work.

Received July 25, 2014; accepted for publication February 06, 2015; available online without subscription through the open access option.

1066-5099/2015/$30.00/0

This article has been accepted for publication and undergone full peer review but has not been through the copyediting, typesetting, pagination and proofreading process which may lead to differences between this version and the Version of Record. Please cite this article as doi: 10.1002/stem.2001.

Key words. Embryonic stem cells • Progenitor cells • Neural differentiation • Proliferation • Self-renewal • Neural stem cell

ABSTRACT

Chromodomain helicase DNA-binding protein 2 (CHD2) has been associated with a broad spectrum of neurodevelopmental disorders, such as autism spectrum disorders and intellectual disability. However, it is largely unknown whether and how CHD2 is involved in brain development. Here, we demonstrate that CHD2 is predominantly expressed in Pax6$^+$ radial glial cells (RGs) but rarely expressed in Tbr2$^+$ intermediate progenitors (IPs). Importantly, the suppression of CHD2 expression inhibits the self-renewal of RGs and increases the generation of IPs and the production of neurons. CHD2 mediates these functions by directly binding to the genomic region of *repressor element 1-silencing transcription factor (REST)*, thereby regulating the expression of REST. Furthermore, the overexpression of REST rescues the defect in neurogenesis caused by CHD2 knockdown. Taken together, these findings demonstrate an essential role of CHD2 in the maintenance of the RGs self-renewal levels, the subsequent generation of IPs, and neuronal output during neurogenesis in cerebral cortical development, suggesting that inactivation of CHD2 during neurogenesis might contribute to abnormal neurodevelopment. STEM CELLS *2014; 00:000–000*

INTRODUCTION

Neurogenesis is an essential process during embryonic cortical development that includes the proliferation and differentiation of neural progenitor cells (NPCs). In the developing cortex, two major types of NPCs are found in the proliferative zones: Pax6$^+$ radial glial cells (RGs) and Tbr2$^+$ intermediate progenitors (IPs). RGs, which are located in the ventricular zone (VZ), divide symmetrically to self-amplify or generate either a neuron or an IP via asymmetrical division [1, 2]. IPs, which is mainly found in the subventricular zone (SVZ), divides symmetrically to generate neurons after one to three amplification divisions. Furthermore, the proliferation of progenitor cells is tightly regulated by both intrinsic and extrinsic factors to control the development of the cerebral cortex. An abnormality in any process may result in improper brain development. For example, the overex-

pression of Trnp1 (TMF1-regulated nuclear protein 1) *in vivo* increases the number of $Pax6^+$ progenitor cells, whereas the knockdown of Trnp1 increases the number of $Tbr2^+$ cells and induces folding of the cerebral cortex [3]. Axin, an essential protein related with neurogenesis by interacting with various signaling proteins, promotes the generation and amplification of IPs but has no significant effect on RGs [4]. Although an increasing number of molecules are involved in the proliferation of progenitors, how neurogenesis is regulated at the molecular and cellular levels during the development of the cerebral cortex remains largely unknown.

Chromodomain helicase DNA-binding protein (CHD) is a member of the ATP-dependent chromatin remodeling family and is crucial for both the assembly and regulation of chromatin. An increasing body of evidence demonstrates that the CHD protein plays instructive and programmatic roles during development [5] and may act as a facilitator of lineage specification [6]. For example, the loss of CHD5 blocks neuronal differentiation and results in an accumulation of undifferentiated progenitors [7], whereas CHD4 depletion promotes astrogenesis without affecting neuronal differentiation in the developing neocortex [8]. CHD7, a candidate gene of CHARGE (*c*oloboma of the eye, *h*eart defects, *a*tresia of the choanae, severe *r*etardation of growth and development, *g*enital abnormalities, and *e*ar abnormalities) syndrome, promotes adult neurogenesis via stimulating the expression of the Sox4 and Sox11 genes [9]. CHD8, an autism susceptibility gene, also has an essential role in brain development [10]. However, the functions of other CHD family members in embryonic cortical development are unclear.

CHD2 belongs to the CHD family of chromatin remodelers. CHD2-null mouse embryos demonstrate a general growth delay and die prior to birth, indicating that CHD2 plays important roles in mammalian development and long-term survival [11]. Haploinsufficiency for CHD2 causes scoliosis and similar features of CHARGE syndrome, such as mental retardation [12]. Deletion of CHD2 in a child results in epilepsy and mental deficiency, indicating an essential role of CHD2 in brain function [13]. Moreover, CHD2 mutations might cause intellectual disability, autism, and epileptic encephalopathies [14-18]. Although a subset of CHD family members play important functions in the maintenance of brain function and the development of the brain, very little is known regarding the role of CHD2 in embryonic neurogenesis. In addition, CHD2 mutations contribute to a broad spectrum of neurodevelopmental disorders, indicating that CHD2 might play an important function in the early development of the neocortex.

With this regard, we investigated the functions of CHD2 in mouse embryonic neurogenesis and explored the underlying molecular mechanism. We found that CHD2 is predominantly expressed in $Pax6^+$ RGs but is rare in $Tbr2^+$ IPs. The knockdown of CHD2 in the embryonic cortex decreases the amplification of RGs and promotes the generation of IPs. Furthermore, depletion of CHD2 results in their premature differentiation. The essential effect of CHD2 in embryonic neurogenesis is performed by stimulating the expression of REST.

Materials and Methods

Plasmid Constructs

The sequences for shRNAs targeting CHD2 are as follows: CHD2-shRNA1, CAAGAACCATCACGATTTAAT; CHD2-shRNA2, GCCTCTAAGAAGGAACGGATA; and CHD2-shRNA3, TCATCCAGGCAGTACTATTAA. CHD2-shRNA3 was targeted to the 3'UTR of CHD2. The CHD2-shRNAs were subcloned into the pSicoR-GFP vector, which was kindly provided by Dr. Wanzhu Jin (Institute of Zoology, Chinese Academy of Sciences). CHD2 cDNA was amplified by PCR and subcloned into pCDH, which was also provided by Dr. Wanzhu Jin. Full-length CHD2 and three different fragments (1-400 aa, 401-1000 aa, and 1000-1825 aa) were amplified from mouse CHD2 cDNA by PCR and subcloned into pCMV-Tag 2 to generate a Flag-tagged expression plasmid. The Flag-tagged fragments and full-length CHD2 were also amplified and cloned into pCDH for lentivirus packaging.

Antibodies

The following primary antibodies were used for immunohistochemistry staining or western blotting analyses: rabbit monoclonal anti-CHD2 (1:1000, Abcam); mouse monoclonal anti-BrdU (1:1000, Millipore); rat monoclonal anti-BrdU (1:1000, Abcam); mouse monoclonal anti-Pax6 (1:100, DSHB); mouse monoclonal anti-Nestin (1:200, Millipore); mouse monoclonal anti-SOX2 (1:500, RD); mouse monoclonal anti-β-actin (1:2000, Proteintech); rabbit monoclonal anti-pax6 (1:1000, Millipore); rabbit monoclonal anti-Tbr2 (1:1000, Abcam); rabbit monoclonal anti-Flag (1:1000, Sigma); rabbit monoclonal anti-tuj1 (1:1000, Sigma); and rabbit monoclonal anti-Ki67 (1:1000, Abcam).

NPC Cultures

Pregnant ICR mice purchased from Vital River Laboratories were used for the isolation of embryonic neural progenitor cells. Briefly, the dorsal telencephalon of E12 ICR embryos was digested in papain (Worthington) for 5 min at 37°C and mechanically dissociated using pipetting tips. Next, the mixture was washed three times with high-glucose DMEM (Gibco) for 5 min at 1100 rpm. Finally, the purified NPCs were plated at a density of 50,000 cells/ml onto acid-treated glass coverslips (Deckglaser) or 48-well plates (Corning, 200 μl/well) in proliferation media for the subsequent experiments. All of the glass coverslips (Deckglaser) and plates (Corning) were coated with poly–L-ornithine (Sigma, 10 μg/ml) and laminin (Sigma, 5 μg/ml).

The proliferation media consisted of NeuroBasal-A medium / DMEM/F12 (Invitrogen) with penicillin-streptomycin-glutamine (Invitrogen), GlutaMAX (Invitrogen, 0.5%), non-essential amino acids (Invitrogen,

1%), B27 supplement (Invitrogen, 2%), bFGF (Invitrogen, 5 ng/ml), and EGF (Invitrogen, 5 ng/ml). The differentiation media consisted of low-glucose DMEM (Gibco) with penicillin-streptomycin-glutamine, 2% B27 supplement, and 1% fetal bovine serum (Invitrogen). For cell proliferation and differentiation, the medium was changed every other day for four days.

Lentivirus Production and Infection

Briefly, lentiviral DNA was transfected into HEK293FT cells with packaging plasmids mediated by GenEscort^{TM}I (Wisegen). The medium with lentivirus was harvested at 24 h, 48 h, and 72 h post-transfection and centrifuged at 3000 rpm for 5 min to eliminate cell debris. The titer of virus was detected in 293FT. Generally, we acquired 0.5-1×10^6 lentiviral particles / ml. Virus was added into the medium according MOI (multiplicity of infection) =5 and incubated overnight. After 2-4 days culture, infected NSC were used for further analysis including RT-PCR, western blot, and immunostainning.

Immunostaining

Immunostaining for cultured cells was performed as follows: the cells were washed with PBS (Invitrogen), fixed in 4% PFA, blocked in 5% BSA (Sangon, in 0.1% PBST), incubated with primary antibodies overnight at 4ºC, and visualized using secondary antibodies.

For the immunostaining of brain sections, pregnant female mice were first injected with 100 mg/kg BrdU (Sigma-Aldrich) via i.p. 2 h or 24 h prior to being killed. Next, the embryonic brains were obtained, fixed in 4% PFA for 24 h at 4ºC, and incubated with 30% (w/v) sucrose in PBS at 4°C for 24 h. Next, the brains were embedded in Tissue-Tek (Sakura) at -20ºC until the immunohistochemical (IHC) analyses. Coronal sections (15 µm) were acquired using a freezing microtome (Leica, CM1950) and attached to pretreated slides. IHC was performed on 15-µm-thick coronal brain sections. Briefly, the brain sections were washed once with 0.1 M PBS, pH 7.4, fixed with 4% PFA for 20 min, and washed three times with PBST (0.1% TritonX-100 in 0.1 M PBS) for 10 min. Next, the brain slices were incubated in blocking buffer (5% bovine serum albumin in 1% PBST) for 1 h at room temperature. Alternatively, when IHC was required for BrdU visualization, the brain sections were fixed with 4% PFA and washed three times with PBST (1% TritonX-100 in 0.1 M PBS) for 10 min. Sequentially, the sections were incubated in ice-cold 1 N HCl for 10 min, in 2 N HCl for 10 min at room temperature, and in 2 N HCl for 20 min at 37°C. After three times washing with PBST, the sections were then incubated with blocking solution as previously described. The brain slices were incubated in primary antibodies overnight at 4°C, washed three times with PBST for 10 min, and incubated with secondary antibodies conjugated to Alexa Fluor dyes (1:1000 dilution; Jackson) in PBST buffer for 1 h at room temperature on a platform shaker. The brain sections were washed three times for 10 min in PBST prior to incubation with DAPI for 1 min, and then washed three times with PBST for 3× 5 min. Unless otherwise stated, all of the IHC procedures were performed at room temperature.

In Utero Electroporation

ICR pregnant female mice were purchased from Vital River Laboratories for in utero electroporation. The detailed protocols have been previously described [19]. Briefly, plasmids were injected into E13.5 embryonic mouse brains with a GFP-expressing plasmid known as Venus at a 3:1 ratio. For cell proliferation analysis, the mice were intraperitoneally (i.p.) injected with BrdU (100 mg/kg) 3 days after electroporation and killed 2 h later. For cell cycle exit analysis, the pregnant mice were treated with BrdU for 24 h before euthanasia. For BrdU dating experiments, the pregnant mice were treated with BrdU 24h after being electroporated and killed 5 days later.

RT-PCR

The total RNA from brain tissue or cells was extracted using the Total RNA Kit (TIANGEN) according to the manufacturer's instructions. First-strand cDNA synthesis was performed using the FastQuant RT Kit (with DNase, TIANGEN). The primers used for real-time PCR were the following: *CHD2* Forward, GACAGTGATTCAGATACTGAGTCTAAG;

Reverse, CTCGGCATCCGTGAAGCCCTCCACAAG; *REST* Forward, AGCGAGTACCACTGGAGGAA; Reverse, CTGAATGAGTCCGCATGTGT; *Pax6* Forward, GCGACTCCAGAAGTTGTAAGCA; Reverse, CTGCCCGTTCAACATCCTTA; *Celsr3* Forward, ATGCTAGGAGAAGCATCCGC; Reverse, GGATCTCTCACCCTGACCCT ; *Ngn2* Forward, AACTCCACGTCCCCATACAG; Reverse, GTGAGGCGCATAACGATGCT; *Mash1* Forward, GCGGCCAACAAGAAGATGAG; Reverse, ATCCCTCGTCGGAGGAGTAG; *Pten* Forward, TGTGGTCTGCCAGCTAAAGGT; Reverse, ACATGAACTTGTCCTCCCGC[20]; and *β-actin* Forward, GGTGGGAATGGGTCAGAAGG; Reverse, AGGAAGAGGATGCGCCAGTG [21].

Western Blotting Analyses

Protein extracts were obtained by lysing the cells/tissue in RIPA (Solarbio) buffer (supplemented with 10 mM PMSF and cocktail). Next, 100 µg of proteins (in 1× loading buffer) were loaded onto SDS-PAGE gels (6%-12%) and transferred onto nitrocellulose or PVDF membranes. The membranes were incubated with primary antibodies, and the primary antibodies were visualized using IRDye® 800CW or 680CW (LI-COR) donkey anti-mouse or anti-rabbit secondary antibodies.

Chromatin immunoprecipitation

In this study, Flag and CHD2 antibody was used for the chromatin immunoprecipitation (ChIP) assay. The cells were treated with 1% formaldehyde at room tempera-

ture for 15 minutes, and 2.5 M glycine was then added to terminate the reaction. After the cells were rinsed three times with cold PBS, the cells were harvested in lysis buffer 1 (50 mM HEPES-KOH [pH 7.5], 140 mM NaCl, 1 mM EDTA [pH 8.0], 10% glycerol, 0.5 % NP-40, 0.25% Triton, Roche protease inhibitor cocktail, and 1 mM PMSF) and then resuspended in lysis buffer 2 (10 mM Tris-HCl [pH 8.0], 200 mM NaCl, 1 mM EDTA [pH 8.0], 0.5 mM EGTA [pH 8.0], Roche protease inhibitor cocktail, and 1 mM PMSF). After centrifugation, each sample was resuspended and sonicated in lysis buffer 3 (10 mM Tris-HCl [pH 8.0], 1 mM EDTA [pH 8.0], 0.5 mM EGTA [pH 8.0], Roche protease inhibitor cocktail, and 1 mM PMSF). The lysates were incubated with 50 µl of Dynabeads Protein A (Invitrogen), which was preloaded with 1 µg antibody overnight at 4°C. After the cells were washed 5 times with wash buffer (50 mM HEPES-KOH [pH7.5], 500 mM LiCl, 10 mM EDTA [pH 8.0], 1% NP-40, and 0.7% sodium deoxycholate), the Dynabeads Protein A were heated at 65°C at least 4h to reverse the covalent histone-DNA bonds. The DNA was extracted using the DNA Gel Extraction Kit, and real-time PCR was performed. The primers used for real-time PCR were the following: *REST* coding sequence forward, TTTGCAGGAGAACGCCC; reverse, CTGAAATGCTGGCAGTCACC; *REST* promoter 1K forward, AAGGTCTCACTTTGTAGCTATGGCT; reverse, ACAGAGGCAGGAGGATTGCTG; And *REST* promoter 2K forward, CTGGCCTCAGACTAGCTATG; reverse, GAGTGTTGGTCTTACAGGT.

Cell pair analysis

E13.5 embryos were electroporated with CHD2-shRNA or control plasmid. At E14.5, the electroporated regions were isolated and dissociated in papain (Worthington) for 5 min at 37°C. Next, the cells was washed three times with high-glucose DMEM (Gibco) for 5 min at 1100 rpm and screened by 40 µm filter twice. Then GFP positive cells were sorted by fluorescence-activated cell sorting (FACS). The sorted cells were plated into 12-well plates, which were pre-coated with poly-L-ornithine/laminin at a clonal density and cultured in proliferating medium. The immunostaining was performed 24 h later.

Image Acquisition and Statistical Analysis

All images were acquired using a confocal Zeiss LSM780 microscope and further analyzed with Adobe Photoshop and Image Pro Plus. The statistical analyses were performed using one-way ANOVA or T-test. All bar graphs are shown as the means±SEM.

RESULTS

Endogenous CHD2 is expressed in neurogenic regions and specifically enriched in radial glial progenitors during cerebral cortical development

To investigate whether CHD2 plays an important role in embryonic neurogenesis, we first assessed the distribution of CHD2 in the developing forebrain from E12 to E18. The immunoreactivity of CHD2 was prominent in the nucleus of progenitors in the VZ/SVZ and of newborn neurons in the CP (Fig. 1A,B,C; Supporting information Fig.1). Importantly, CHD2 was predominantly expressed in a subset of $Pax6^+$ RGs (Fig. 1D), whereas it was rarely expressed in $Tbr2^+$ IPs (Fig. 1E). To further demonstrate the expression of CHD2 in RGs, we isolated neural progenitors from E12, E15, and E18 brains and cultured into neurospheres. RT-PCR results showed that the expression of CHD2 was down-regulated when Pax6, the RGs marker, reduced (Fig. 1F). Simultaneously, CHD2 immunoreactivity was also detected in Sox2-positive cells and Nestin-positive progenitor cells (Fig. 1G, 1H). Taken together, endogenous CHD2 is expressed in neurogenic regions and is abundant in RGs but largely absent in IPs during cerebral cortical development.

To confirm that CHD2 is also expressed *in vitro*, immunostaining studies were performed on both HEK293FT cells expressing Flag-tagged CHD2 and cultured neurospheres. Consistent with these studies, CHD2 was also expressed in the nucleus of HEK293FT cells and cultured neurospheres (Fig. 1I, 1J). Moreover, CHD2 was also co-expressed with Sox2, Pax6, and Nestin, demonstrating the expression of CHD2 in progenitors *in vitro* (Fig. 1K).

CHD2 is essential for the development of neocortex and the proliferation of progenitor cells

Given that the expression pattern suggested a potential role of CHD2 in embryonic neurogenesis, we investigated the function of CHD2 using in utero intraventricular microinjections. Three small hairpin RNAs (shRNAs) targeting the 3'UTR or coding sequence of CHD2 mRNA were cloned into pSicoR. Western blotting analyses showed that these three shRNAs could effectively knock down the expression of CHD2 (Fig. 3A). Moreover, the expression of CHD2 was depleted in CHD2 shRNA electroporated cells (Fig. 3B). To detect the role of CHD2 in embryonic neurogenesis, we electroporated CHD2-shRNA or control plasmid with a GFP-expressing vector into E13.5 cerebral cortices and detected the GFP distribution 3 days later. CHD2 knockdown resulted in a significant reduction of GFP-positive cells in the VZ/SVZ. Consistent with these findings, the number of GFP-positive cells in the CP was clearly increased (Fig. 2A, 2B). Moreover, CHD2 overexpression resulted in an ac-

cumulation of GFP-positive cells in the VZ/SVZ and a reduction of GFP-positive cells in the CP (Fig. 2C, 2D). Taken together, these results indicated that CHD2 plays an essential role during cortical development from E13.5 to E16.5, which is in the neuronogenetic interval starting on E10.5 and ending on 16.5 in mice.

Because the difference in GFP-positive cells was clearly observed in the VZ/SVZ, which is the region where progenitor cells are enriched, we hypothesized that CHD2 regulates the proliferation of progenitors in embryonic neurogenesis. To test this hypothesis, we injected BrdU into electroporated pregnant animals 2 h prior to euthanasia. Interestingly, CHD2 knockdown resulted in a significant reduction in BrdU incorporation at E16.5 (Fig. 2E, 2F), whereas CHD2 overexpression resulted in more BrdU-positive cells compared to the control (Fig. 2G, 2H), suggesting that CHD2 is required for the proliferation of progenitors.

To further confirm the role of CHD2 in the proliferation of progenitors, primary progenitors were infected with recombinant lentivirus expressing CHD2-shRNA or CHD2, and the proliferative capability of the cells was analyzed using EdU labeling. Consistent with these findings *in vivo*, progenitors infected with CHD2-overexpressing lentivirus showed increased proliferation, whereas progenitors infected with CHD2-shRNA lentivirus exhibited reduced proliferation (Fig. 3C,D,E,F). Moreover, the clones that were initially generated from a single infected cell were much smaller in the CHD2-knockdown cells compared to the control (Fig. 3G, 3H).

Taken together, the data showed that CHD2 plays an essential role during cortical development, particularly in progenitor proliferation. Both *in vivo* and *in vitro* results revealed that CHD2 promotes the proliferation of progenitors.

CHD2 promotes the proliferation of RGs and inhibits the generation of IPs

There are two major types of progenitors, RGs and IPs, in the VZ/SVZ. How CHD2 regulates these two types of progenitors is unknown. For this purpose, we examined the proportion of $Pax6^+GFP^+$ cells and $Tbr2^+GFP^+$ cells. Consistent with the expression of CHD2 in a subset of $Pax6^+$ cells, CHD2 knockdown significantly reduced the number of $Pax6^+$ cells (Fig. 4A, 4D). Simultaneously, the number of $Tbr2^+$ cells increased (Fig. 4C, 4F). In contrast, CHD2 overexpression increased the number of $Pax6^+$ cells (Fig. 4B, 4E). These results indicated that CHD2 is necessary for the self-renewal of RGs and the generation of IPs.

To further clarify the functional roles of CHD2 on RGs and IPs, the proliferation of RGs and IPs was assessed using BrdU labeling 2 h before the pregnant mice were euthanized. When CHD2 was knocked down, the amplification of RGs, which were $Pax6^+$and $BrdU^+$, was significantly reduced, whereas the proliferation of IPs, which were marked by Tbr2 and BrdU, has no significant variation (Fig. 4G,H,I,J). Consistent with this finding, the amplification of RGs increased when CHD2 was overexpressed. These results showed that CHD2 promotes the proliferation of RGs but not of IPs. Moreover, cell-pair analysis *in vitro* showed that CHD2 knockdown in RGs decreased the number of RG-RG cell pairs, whereas the RG-IP cell pairs were increased (Fig. 4K, 4L). These findings revealed that the knockdown of CHD2 inhibites the self-amplification of RGs and promotes the generation of IPs.

Taken together, these findings showed that CHD2 has an essential role in the self-renewal and maintenance of radial glial progenitors during embryonic neurogenesis. The magnitude of the CHD2 effect is substantial because its reduction promotes the generation of IPs and potentially the production of neurons.

CHD2 knockdown promotes neuronal production

Because IPs are considered the major resource of neuronal production [1] and CHD2 knockdown promotes the generation of IPs, we investigated the effect of CHD2 on neuronal production. To this end, BrdU was administered 2 days later at E15.5 to trace the proliferated cells. At E16.5, the pregnant mouse was euthanized, and the embryonic brains were collected for analysis. The brain sections were stained with antibodies for GFP, BrdU, and Ki67. The ratio of $GFP^+/BrdU^+/Ki67^+$ cells was significantly reduced in the CHD2-knockdown brains. However, the percentage of $GFP^+/BrdU^+/Ki67^-$ cells that exited the cell cycle was significantly increased (Fig. 5A, 5B). Compared with control, more $Tuj1^+$ neurons were detected in CHD2-shRNA lent virus infected groups *in vitro* (Supporting Information Fig. 2A, 2B). In support of these findings, more GFP^+Tuj1^+ cells were investigated in CHD2-knockdown brains, indicating that a reduction of CHD2 promotes neuronal production (Fig. 5C, 5D). Taken together, these results revealed that more cells exited the cell cycle and differentiated into neurons when CHD2 was knocked down. The effect of CHD2 on neuron production was further verified by BrdU birth dating experiment. The embryos were electroporated at E13.5, injected BrdU at E14.5 and collected at E18.5 (Fig. 5E). At E18.5, most GFP^+ cells were located in the CP in both control and CHD2-shRNA electroporated brains. Compared with control, more $BrdU^+GFP^+$ cells were observed in CP when CHD2 was knockdown (Fig.5F, 5G). The result indicated that more progenitor cells were differentiated into neurons when CHD2 was reduced. Together, the knockdown of CHD2 inhibits the self-renewal of RGs and subsequently promotes the generation of IPs and the production of neurons.

CHD2 regulates embryonic neurogenesis by promoting the expression of REST

To investigate the molecular mechanism underlying CHD2 regulation in embryonic neurogenesis, the direct target gene of CHD2 that plays a role in embryonic neurogenesis needs to be identified. For this purpose, ex-

pression data from the Cancer Genome Atlas Project (TCGA) was analyzed. Interestingly, REST, RE1-Silencing Transcription factor, which is known as a neuron-restrictive silencer factor, is positively correlated with CHD2 expression. The expression of REST was obviously down-regulated from E12 to E15 (Fig. 6A), indicating a potential role of REST in neurogenesis. When CHD2 was knocked down, the expression of REST was also reduced (Fig. 6B), while the expression of REST was up-regulated when CHD2 is over expressed (Supporting Information Fig. 1B), suggesting REST may be the candidate gene that is regulated by CHD2 during neurogenesis. Meanwhile, REST target genes, Celsr3, which is required for neurite growth [22], as well as Mash1 and Ngn2 [21, 23], which are lineage-specific genes, were detected. The expression of REST target genes was up-regulated by RNAi-mediated CHD2 knockdown, and down-regulated by CHD2 overexpression (Suppporting Information Fig. 1A, 1C). To test whether REST overexpression in the developing neocortex might result in similar redistribution of electroporated cells as observed in CHD2 overexpression. REST overexpressing plasmid and control were electroporated. Similarly, the number of GFP-positive cells in the SVZ/VZ was increased, whereas the number of GFP-positive cells in the CP was significantly reduced when REST were overexpressed in the developing cortex (Fig. 6C, 6D). To test whether *REST* is a direct target gene of CHD2, Chromatin immunoprecipitation (ChIP) experiments were performed in primary NSC to detect the binding of CHD2 to *REST* (Fig. 6E). The results showed that not only promoter but also coding region of *REST* were occupied by CHD2. When CHD2 was knocked down, the binding enrichment of *REST* was reduced (Fig. 6F), whereas more binding was detected in CHD2 overexpressing NSC (Fig.6G). To identify the functional domain of CHD2 that regulates the expression of REST, FLAG-tagged CHD2 fragments and full-length CHD2 were used for ChIP experiments. Results showed that CHD2 promotes the expression of REST through the chromatin-binding domain and the DNA binding domain (Fig. 6H, 6I). To further illustrate the relationship between CHD2 and REST in brain development, rescue experiments were performed with REST overexpression when CHD2 was silenced. As mentioned above, CHD2 knockdown decreased the percentage of GFP^+ cells in the VZ/SVZ and increased the number of GFP^+ cells in the CP. Importantly, the overexpression of REST rescued the abnormal distribution of GFP^+ cells caused by CHD2 knockdown (Fig. 7A, 7B). Furthermore, the defect of RGs amplification caused by CHD2 knockdown could be rescued by REST overexpression (Fig. 7C, 7D).This investigation suggested that CHD2 controls embryonic neurogenesis by regulating REST expression.

DISCUSSION

Neurogenesis is an essential process for brain development that is generally accompanied by a gradual loss of progenitor potential and the appearance of specific neuronal traits [24]. Thus, the maintenance of the progenitor pool is important for the persistent production of neurons. A reduced number of IPs caused by the precocious depletion of RGs ultimately results in the production of fewer neurons, resulting in a smaller cortex [25]. In this study, we reported that the chromatin remodeler CHD2 plays an essential role in governing the neurogenic potential of progenitors. The depletion of CHD2 inhibits the self-renewal of RGs and subsequently promotes the generation of IPs and the production of neurons in the short-term. Both the decrease in the amplification of RGs and the increase in the transition from RGs to IPs contribute to the reduction of RGs when CHD2 is silenced. Taken together, our data demonstrated that CHD2 plays an important role in embryonic neurogenesis by maintaining the self-renewal capacity of RGs and by preventing the precocious depletion of the progenitor pool.

We observed that CHD2 knockdown increased the number of IPs, whereas no significant effect on the amplification of IPs was observed when BrdU was administered 2 h later. The data indicated that the increase in IPs mainly resulted from the transition of RGs to IPs but not the self-amplification of IPs. In addition, CHD2 expression is largely absent in IPs, and the knockdown of CHD2 has no direct effect on IPs. Thus, our results demonstrated that CHD2 knockdown altered the composition of the progenitor pool, resulting in a relative decrease in RGs and an increase in IPs. This shift was further confirmed using cell pair analysis *in vitro,* which showed that CHD2 knockdown inhibit the amplification of RGs and promote the generation of IPs from RGs. Because RGs can self-renew and maintain the progenitor pool during cortical development, a decrease in RGs induced by CHD2 knockdown may result in a transient enlargement but a rapid depletion of the progenitor pool.

Chromatin regulators are commonly thought to facilitate lineage specification rather than be directly involved in the process [6]. Although IPs are a major source of neuronal production, IPs are generated from RGs. Thus, the role of CHD2 on neuron production needs to be clarified. The suppression of CHD2 results in the generation of more IPs. Consistent with this finding, the number of cells exiting the cell cycle and labeled with Tuj1 was increased at E16.5, indicating that CHD2 reduction promotes neuronal differentiation. Thus, the transient increase in neuronal production was also a primary effect of CHD2 knockdown on the proliferation of RGs and the transition from RG to IPs. Simultaneously, CHD2 is also expressed in immature neurons. The other roles of CHD2 in neuronal differentiation remain unknown.

In the developing neocortex, neurogenesis occurs from E10.5 to E16.5. To study the role of CHD2 in neurogenesis, we electroporated target plasmids at E13.5 and analyzed the phenotype at E16.5. Our data demonstrated that CHD2 is a pivotal regulator of the self-renewal of RGs as well as of the generation of neurons.

However, these results only reflect a snapshot of the progenitor pool at E16.5. Thus, to emphasize the functions of CHD2 in maintaining the size of the progenitor pool, tracing experiments need to be performed.

The binding of CHD2 to the REST genomic region suggests that it contributes to the silencing of neuronal genes in the proliferation stage but not in the differentiation stage. The role of REST in embryonic stem cell is controversial. Singh et. al showed that REST maintains the self-renewal and pluripotency of embryonic stem cells [21]. However, inconsistent results were put forward [26-28]. The discrepancy indicates that the function of REST is restricted by multiple factors. Yamada et.al found that REST promotes ESC differentiation but is not required for their maintenance [29]. Soldati et. al showed that REST is not essential for production of radial glia-like progenitors but is required for their subsequent maintenance and neural differentiation [30]. As a repressor of neuronal genes, the expression of REST is downregulated in the transition from neural progenitor to neuronal differentiation during brain development [23, 31, 32]. The persistently expression of REST blocks the radial migration and delays neuronal differentiation [33]. Furthermore, REST plays important role in neural stem cell proliferation and differentiation mediated by *ZNF335* [34]. Recently, REST has been reported to play important functions in preventing cognitive decline and Alzheimer's disease in the aged brain [35]. Briefly, REST is an essential regulator of neurogenesis during development and cognitive prevention during aging. In this study, we identified a new upstream regulator of REST, CHD2. The regulation of REST by CHD2 is not mediated by H3K4me3 modification (data not shown) but by binding to the genomic region of REST. In addition, the binding domain of CHD2 may be the chromatin and DNA-binding domains. Moreover, REST can rescue the abnormal cell distribution caused by CHD2 depletion. Thus, CHD2 regulates embryonic neurogenesis by promoting the expression of REST.

Interestingly, several studies have suggested that mutations in CHD2 contribute to a broad spectrum of neurodevelopmental disorders [14, 15, 36]. For example, two mutations in the SNF2-related helicase/ATPase domain of CHD2 were correlated with epileptic encephalopathy. A CHD2 frameshift mutation was associated with intellectual disability. Mutations of CHD2 result in a broad spectrum of neurodevelopment disorders, indicating that CHD2 may play important functions during the early stage of brain development. Thus, the exploration of the role of CHD2 in embryonic neurogenesis is particularly well-suited for the study of CHD2-related diseases.

Taken together, the data show that CHD2 plays an essential role in maintaining the progenitor pool. The depletion of CHD2 may disturb the balance between the proliferation and differentiation of RGs and result in a rapid depletion of the progenitor pool. The regulatory function of CHD2 in embryonic neurogenesis may provide insights into the molecular mechanisms underlying neurogenic disorders.

CONCLUSION

In summary, we find that CHD2 is predominantly expressed in most $Pax6^+$ radial glial cells (RGs) but rarely expressed in $Tbr2^+$ intermediate progenitors (IPs). *In vivo* evidences suggest that the suppression of CHD2 expression inhibits the self-renewal of RGs and increases the generation of IPs and the production of neurons. Furthermore, CHD2 mediates these functions by directly binding to the genomic region of *repressor element 1-silencing transcription factor (REST)*, thereby regulating the expression of REST. Our study clearly demonstrated the role of CHD2 in embryonic neurogenesis and brain development and may provide new insights into the molecular mechanisms underlying the pathogenesis of neurodevelopmental disorders.

ACKNOWLEDGMENTS

This work was supported by grants obtained from the National Key Basic Research Program of China (2015CB964500, 2014CB964903 and 2014CB964602), the National Science Foundation of China (31371477 and 31300894), and the Strategic Priority Research Program (XDA01020301).

CONFLICT OF INTEREST

The authors declare that they have no conflict of interest.

AUTHOR CONTRIBUTIONS

T.S., F.J., Z.Y., and J.J. conceived and designed the experiments; T.S. and F.J. performed the experiments and analyzed the data; F.J., T.S., and J.J. prepared the manuscript.

REFERENCES

1 Pontious A, Kowalczyk T, Englund C, et al. Role of intermediate progenitor cells in cerebral cortex development. Dev Neurosci 2008; 30: 24-32.

2 Imayoshi I and Kageyama R. bHLH factors in self-renewal, multipotency, and fate choice of neural progenitor cells. Neuron 2014; 82: 9-23.

3 Stahl R, Walcher T, De Juan Romero C, et al. Trnp1 regulates expansion and folding of the mammalian cerebral cortex by control of radial glial fate. Cell 2013; 153: 535-49.

4 Fang WQ, Chen WW, Fu AK, et al. Axin directs the amplification and differentiation of intermediate progenitors in the developing cerebral cortex. Neuron 2013; 79: 665-79.

5 Ho L and Crabtree GR. Chromatin remodelling during development. Nature 2010; 463: 474-84.

6 Holmberg J and Perlmann T. Maintaining differentiated cellular identity. Nat Rev Genet 2012; 13: 429-39.

7 Egan CM, Nyman U, Skotte J, et al. CHD5 is required for neurogenesis and has a dual role in facilitating gene expression and polycomb gene repression. Dev Cell 2013; 26: 223-36.

8 Sparmann A, Xie Y, Verhoeven E, et al. The chromodomain helicase Chd4 is required for Polycomb-mediated inhibition of astroglial differentiation. EMBO J 2013; 32: 1598-612.

9 Feng W, Khan MA, Bellvis P, et al. The chromatin remodeler CHD7 regulates adult neurogenesis via activation of SoxC transcription factors. Cell Stem Cell 2013; 13: 62-72.

10 Bernier R, Golzio C, Xiong B, et al. Disruptive CHD8 Mutations Define a Subtype of Autism Early in Development. Cell 2014; 158: 263-76.

11 Marfella CG, Ohkawa Y, Coles AH, et al. Mutation of the SNF2 family member Chd2 affects mouse development and survival. J Cell Physiol 2006; 209: 162-71.

12 Kulkarni S, Nagarajan P, Wall J, et al. Disruption of chromodomain helicase DNA binding protein 2 (CHD2) causes scoliosis. Am J Med Genet A 2008; 146A: 1117-27.

13 Capelli LP, Krepischi AC, Gurgel-Giannetti J, et al. Deletion of the RMGA and CHD2 genes in a child with epilepsy and mental deficiency. Eur J Med Genet 2012; 55: 132-4.

14 Rauch A, Wieczorek D, Graf E, et al. Range of genetic mutations associated with severe non-syndromic sporadic intellectual disability: an exome sequencing study. Lancet 2012; 380: 1674-82.

15 Carvill GL, Heavin SB, Yendle SC, et al. Targeted resequencing in epileptic encephalopathies identifies de novo mutations in CHD2 and SYNGAP1. Nat Genet 2013; 45: 825-30.

16 Pinto D, Delaby E, Merico D, et al. Convergence of genes and cellular pathways dysregulated in autism spectrum disorders. Am J Hum Genet 2014; 94: 677-94.

17 De Rubeis S, He X, Goldberg AP, et al. Synaptic, transcriptional and chromatin genes disrupted in autism. Nature 2014; 515: 209-15.

18 Iossifov I, O'Roak BJ, Sanders SJ, et al. The contribution of de novo coding mutations to autism spectrum disorder. Nature 2014; 515: 216-21.

19 Sanada K and Tsai LH. G protein betagamma subunits and AGS3 control spindle orientation and asymmetric cell fate of cerebral cortical progenitors. Cell 2005; 122: 119-31.

20 Yoshimi A, Goyama S, Watanabe-Okochi N, et al. Evi1 represses PTEN expression and activates PI3K/AKT/mTOR via interactions with polycomb proteins. Blood 2011; 117: 3617-28.

21 Singh SK, Kagalwala MN, Parker-Thornburg J, et al. REST maintains self-renewal and pluripotency of embryonic stem cells. Nature 2008; 453: 223-7.

22 Jorgensen HF, Terry A, Beretta C, et al. REST selectively represses a subset of RE1-containing neuronal genes in mouse embryonic stem cells. Development 2009; 136: 715-21.

23 Ballas N, Grunseich C, Lu DD, et al. REST and its corepressors mediate plasticity of neuronal gene chromatin throughout neurogenesis. Cell 2005; 121: 645-57.

24 Molyneaux BJ, Arlotta P, Menezes JR, et al. Neuronal subtype specification in the cerebral cortex. Nat Rev Neurosci 2007; 8: 427-37.

25 Buchman JJ, Tseng HC, Zhou Y, et al. Cdk5rap2 interacts with pericentrin to maintain the neural progenitor pool in the developing neocortex. Neuron 2010; 66: 386-402.

26 Jorgensen HF, Chen ZF, Merkenschlager M, et al. Is REST required for ESC pluripotency? Nature 2009; 457: E4-5; discussion E7.

27 Jorgensen HF and Fisher AG. Can controversies be put to REST? Nature 2010; 467: E3-4; discussion E5.

28 Buckley NJ, Johnson R, Sun YM, et al. Is REST a regulator of pluripotency? Nature 2009; 457: E5-6; discussion E7.

29 Yamada Y, Aoki H, Kunisada T, et al. Rest promotes the early differentiation of mouse ESCs but is not required for their maintenance. Cell Stem Cell 2010; 6: 10-5.

30 Soldati C, Bithell A, Johnston C, et al. Repressor element 1 silencing transcription factor couples loss of pluripotency with neural induction and neural differentiation. Stem Cells 2012; 30: 425-34.

31 Chong JA, Tapia-Ramirez J, Kim S, et al. REST: a mammalian silencer protein that restricts sodium channel gene expression to neurons. Cell 1995; 80: 949-57.

32 Schoenherr CJ and Anderson DJ. The neuron-restrictive silencer factor (NRSF): a coordinate repressor of multiple neuron-specific genes. Science 1995; 267: 1360-3.

33 Mandel G, Fiondella CG, Covey MV, et al. Repressor element 1 silencing transcription factor (REST) controls radial migration and temporal neuronal specification during neocortical development. Proc Natl Acad Sci U S A 2011; 108: 16789-94.

34 Yang YJ, Baltus AE, Mathew RS, et al. Microcephaly gene links trithorax and REST/NRSF to control neural stem cell proliferation and differentiation. Cell 2012; 151: 1097-112.

35 Lu T, Aron L, Zullo J, et al. REST and stress resistance in ageing and Alzheimer's disease. Nature 2014; 507: 448-54.

36 Neale BM, Kou Y, Liu L, et al. Patterns and rates of exonic de novo mutations in autism spectrum disorders. Nature 2012; 485: 242-5.

See www.StemCells.com for supporting information available online. STEM CELLS *; 00:000–000*

Figure 1. CHD2 is highly expressed in the neurogenic region and specifically enriched in a subset of RGs during cerebral cortical development

(A-C): CHD2 is expressed in the developing cerebral cortex. Brain sections of E12 (A), E15 (B), and E18 (C) mice were stained using anti-CHD2 antibodies (red). The nuclei were stained using DAPI (blue).

(D): CHD2 is detected in a subset of $Pax6^+$ RGs in the E15 cerebral cortex. The arrows indicate cells that are double labeled with CHD2 and Pax6.

(E): CHD2 is largely undetected in $Tbr2^+$ IPs in the VZ/SVZ of the E15 cerebral cortex. The arrowheads indicate $CHD2^-/Tbr2^+$ cells.

(F): The expression of CHD2 is consistent with the expression of Pax6, RGs marker. Progenitors were isolated from the brains of E12 to E18 and cultured into neurospheres. RT-PCR was performed to detect the expression of CHD2 and Pax6 in cultured neurospheres.

(G-H): CHD2 immunoreactivity is present in $Sox2^+$ (G) and $Nestin^+$ (H) progenitors in the VZ/SVZ of the E15 cerebral cortex. The arrows indicate double-positive cells.

(I): CHD2 is expressed in neurospheres cultured *in vitro*. Primary progenitor cells were isolated from the E13 cortex and cultured into neurospheres 2 days later. Immunocytochemical analysis was performed on the neurospheres using antibodies against CHD2. The nuclei were stained using DAPI (blue).

(J): Flag-CHD2 is expressed in HEK293FT cells. HEK293FT cells transfected with the Flag-CHD2 plasmid were stained using anti-Flag (red). The nuclei were stained using DAPI (blue).

(K): CHD2 was co-labeled with Nestin, Pax6, and Sox2 in dissociated progenitor cells.

VZ/SVZ, ventricular zone/subventricular zone; IZ, intermediate zone; CP, cortical plate. Scale bar, 50 μm. Error bars represent SEM based on n=3. At least three sections were used for analysis.

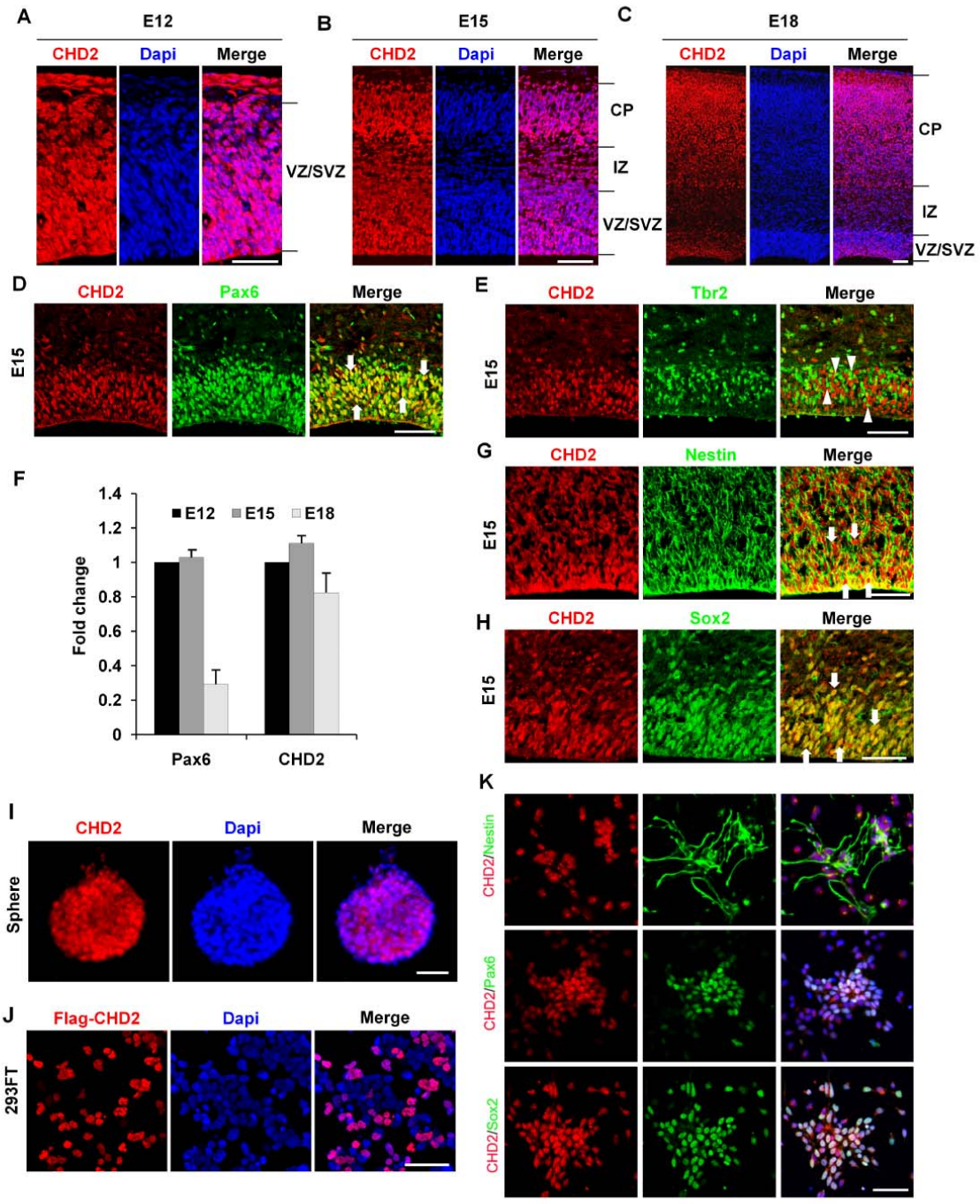

Shen et al., Figure 1

Figure 2. Alteration of CHD2 results in abnormal cell distribution and progenitor amplification.

(A): CHD2 knockdown results in altered cell distribution. E13.5 mouse embryos were electroporated with pSicoR-GFP (Control) and pSicoR-GFP-CHD2 shRNA, and the distribution of GFP^+ cells was investigated at E16.5. The nuclei were stained using DAPI (blue).

(B): The percentage of GFP^+ cells in the VZ/SVZ, IZ, and CP were quantified.

(C): The overexpression of CHD2 *in vivo* results in different cell distributions compared with the control. Either pCDH or pCDH-CHD2 plasmids were electroporated into mouse embryos at E13.5. The distribution of GFP^+ cells was observed at E16.5.

(D): Quantification of GFP^+ cells in the VZ/SVZ, IZ, and CP.

(E): The knockdown of CHD2 decreases the proliferation of progenitors in the VZ/SVZ. In utero electroporation was performed at E13.5, and BrdU was injected into the electroporated pregnant mouse 2 h before the animal was euthanized. The arrows indicate the GFP^+ cells that were also labeled with BrdU in the VZ/SVZ.

(F): Quantification of $BrdU^+GFP^+$ cells in the VZ/SVZ.

(G): The overexpression of CHD2 promotes the amplification of progenitors in the VZ/SVZ. The performance was same with CHD2 knockdown.

(H): Statistical analyses of proliferated cells in (G).

Data are the mean of five litters; error bars indicate SEM. Student's t-test, n.s., not significant; *P<0.05; **P<0.01. Scale bar, 50 μm.

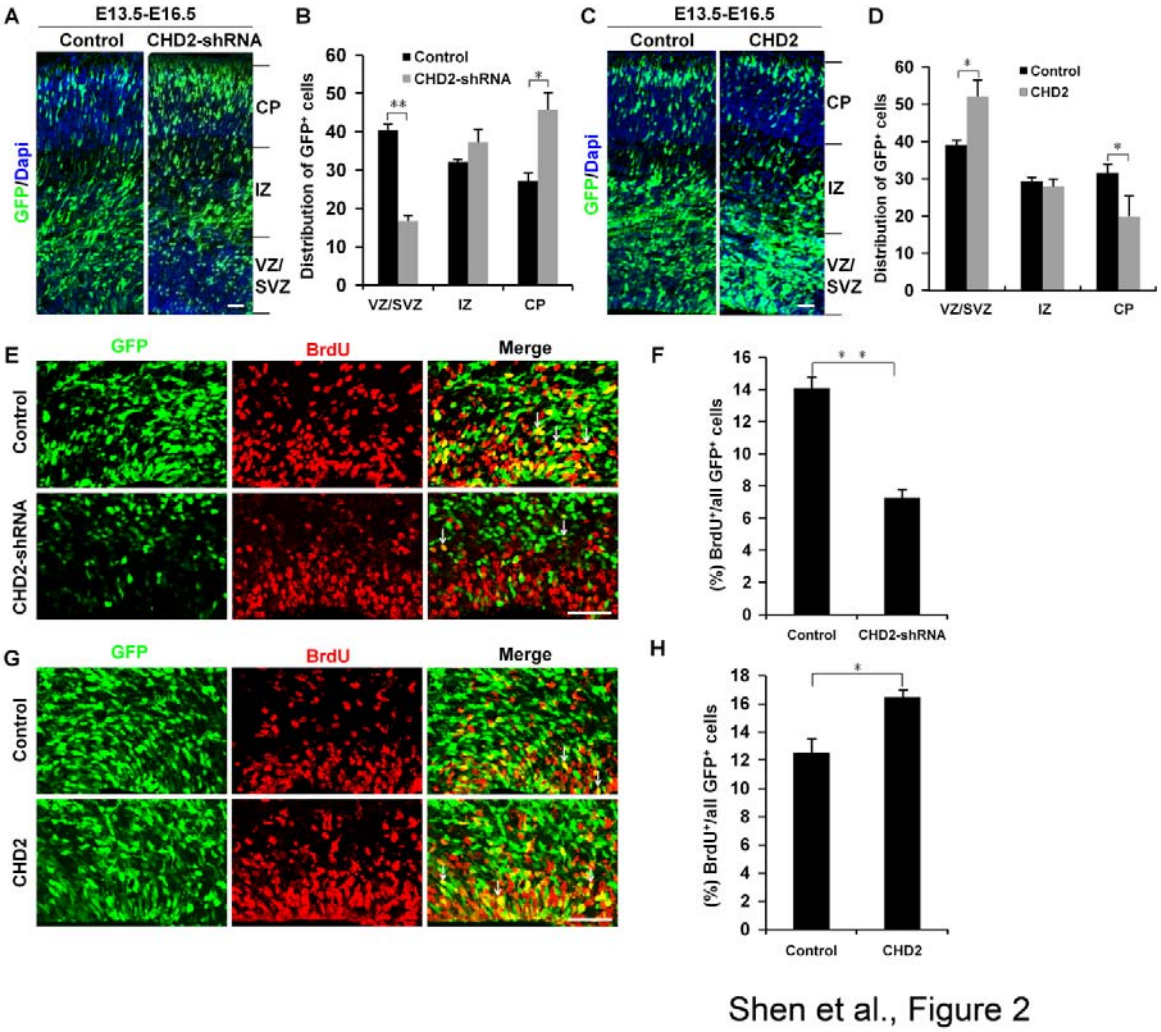

Shen et al., Figure 2

Figure 3. CHD2 regulates the proliferation of progenitors *in vitro*.
(A): The western blotting analysis shows that CHD2 was effectively suppressed using RNA interference. Primary NSCs were infected with control or CHD2 shRNA lentivirus. The cell lysates were probed with anti-CHD2 and β-actin antibodies.
(B): The expression of CHD2 was also effectively suppressed *in vivo*. Scale bar, 10μm.
(C): Proliferation analyses shows that CHD2 depletion inhibited the proliferation of primary progenitor cells. Cells infected with control or CHD2 shRNA lentivirus (GFP) were labeled with EdU (red) and then stained.
(D): Quantitative analysis shows that there was a lower percentage of EdU incorporation in the CHD2-shRNA infected progenitor cells compared to the control cells.
(E): CHD2 overexpression increases the amplification of progenitor cells. Cells infected with control or CHD2 lentivirus were labeled with EdU (red) and then stained.
(F): A higher percentage of EdU incorporation was quantified in CHD2 lentivirus-infected cells compared to the control.
(G): Smaller colonies formed in CHD2 shRNA virus-infected cells. Primary progenitor cells isolated from the E13 cerebral cortex were infected with a low virus titer. Immunostaining for GFP and Tuj1 was performed 7 days later.
(H): The cell number per colony was quantified and compared.
The values represent the means ± SEM based on n=3. Student's t-test, n.s., not significant; *P<0.05; **P<0.01. Scale bar, 50 μm.

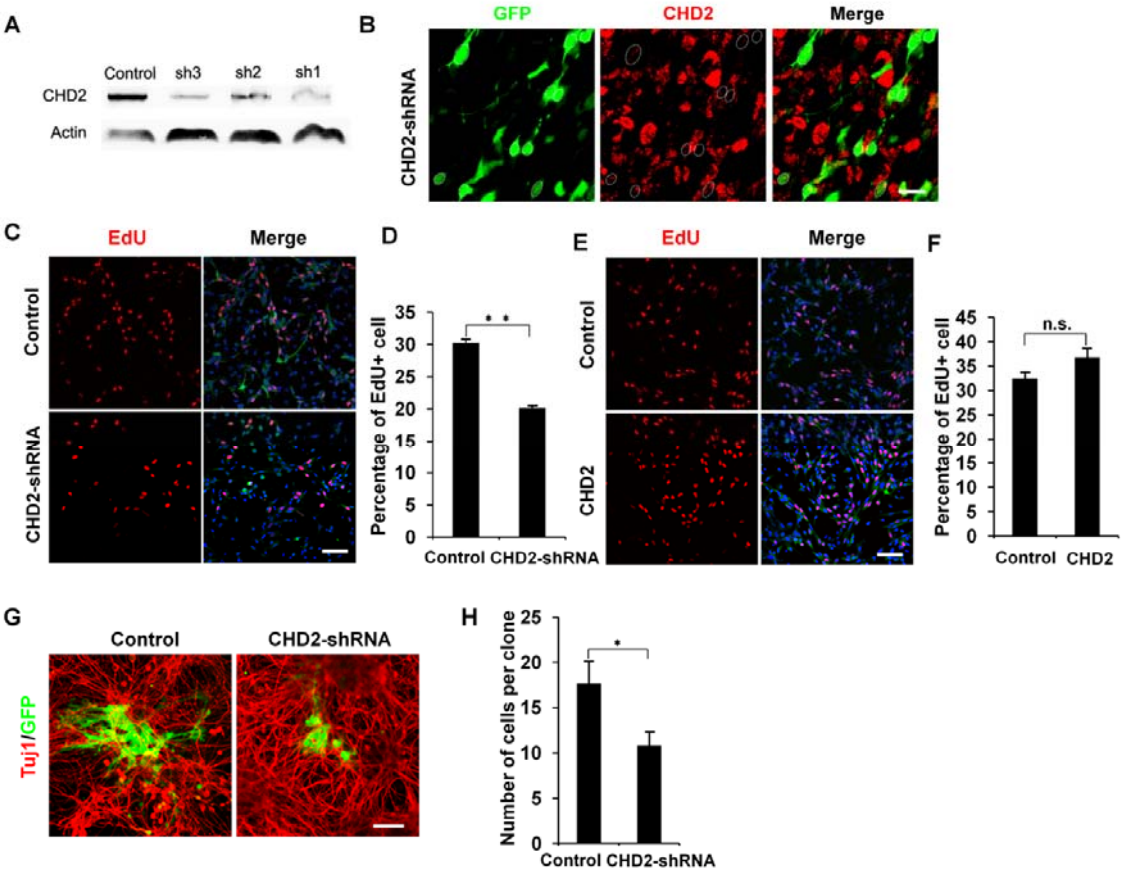

Shen et al., Figure 3

Figure 4. Knockdown of CHD2 inhibits the proliferation of RGs and promotes the generation of IPs *in vivo*

(A): The knockdown of CHD2 decreases the number of RGs. Sections of the cerebral cortex were stained using anti-Pax6 (red). The arrows indicate the $Pax6^+/GFP^+$ cells in the VZ/SVZ.

(B): CHD2 overexpression increases the number of RGs. Sections of the cerebral cortex were stained using anti-Pax6 (red).

(C): CHD2 knockdown results in an increase in IPs. Coronal sections were stained with anti-Tbr2 (red). The arrows indicate the $Tbr2^+/GFP^+$ cells in the VZ/SVZ.

(D): Histogram depicting the percentage of $Pax6^+/GFP^+$ cells within the total GFP^+ cell population in the VZ/SVZ when CHD2 is depleted.

(E): The percentage of $Pax6^+/GFP^+$ cells in the VZ/SVZ when CHD2 is overexpressed.

(F): Percentage of $Tbr2^+/GFP^+$ cells in the VZ/SVZ when CHD2 is knocked down.

(G): The knockdown of CHD2 inhibits the proliferation of RGs. In utero electroporation was performed at E13.5, and BrdU was injected into the electroporated pregnant animal 2 h before euthanasia. Coronal sections were stained using anti-Pax6 (red) and anti-BrdU (pink). The arrows indicate the $GFP^+/Pax6^+/BrdU^+$ cells.

(H): Percentage of $GFP^+Pax6^+BrdU^+$ cells divided by GFP^+Pax6^+ cells.

(I): The knockdown of CHD2 has no significant effect on the proliferation of IPs. Brain sections were stained with anti-Tbr2 (red) and anti-BrdU (pink). The arrows indicate the GFP, Tbr2 and BrdU triple-positive cells.

(J): Percentage of $GFP^+Tbr2^+BrdU^+$ cells within the GFP^+Tbr2^+ cell population.

(K): *In vitro* cell-pair analysis of three types of cell division (RG-RG, IP-IP, RG-IP). The cells were stained using anti-Pax6 (red) and anti-Tbr2 (pink). The GFP^+ pair cells were subjected to further analysis. N=3 independent experiments. Scale bar, 10μm.

(L): CHD2 knockdown inhibits the amplification of RGs and promotes the transition from RGs to IPs *in vitro*. The percentage of GFP^+ cell pairs that are also $Pax6^+$ or $Tbr2^+$ is shown.

Data are the mean of five litters; error bars indicate SEM. Student's t-test, n.s., not significant; *P<0.05; **P<0.01. Scale bar, 50 μm.

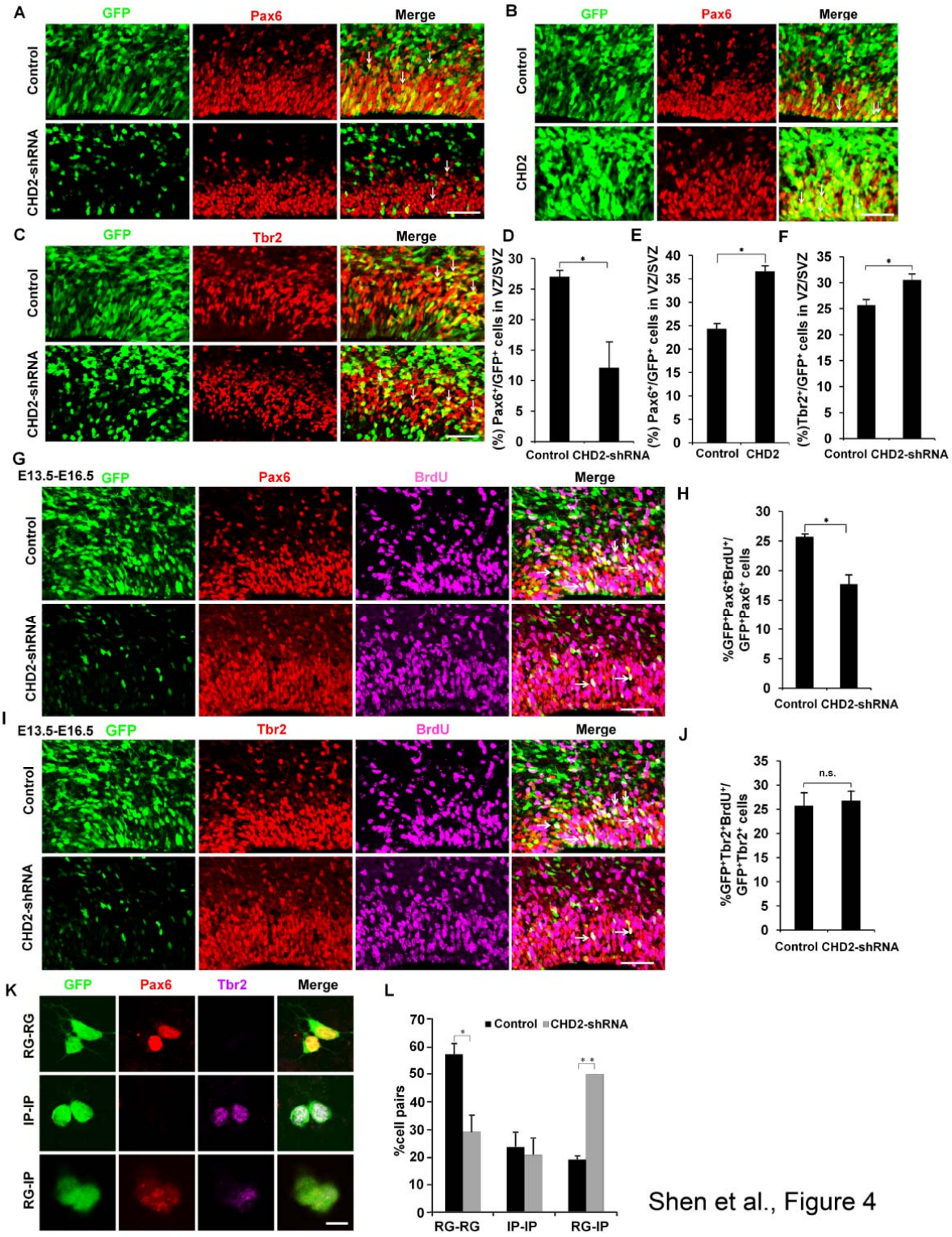

Shen et al., Figure 4

Figure 5. CHD2 knockdown affects neuronal differentiation.
(A): CHD2 knockdown affects cell cycle exit. E13.5 embryos were electroporated with CHD2 shRNA, and BrdU was administered 24 h before the pregnant dams were euthanized at E16.5. Coronal sections were stained with anti-Ki67 (red) and anti-BrdU (pink). The arrows indicate $GFP^+/BrdU^+/Ki67^-$ cells.
(B): Percentage of cells that exit the cell cycle ($GFP^+/BrdU^+/Ki67^-$) in BrdU-labeled GFP^+ cell population.
(C): CHD2 knockdown affects neuronal production. Coronal sections were stained with anti-Tuj1 (red).
(D): The percentage of GFP^+ cells that are also positive for Tuj1 is shown.
(E)Schematic illustration of the BrdU birth dating experimental design. The embryos were electroporated at E13.5, administrated BrdU at E14.5 and collected at E18.5.
(F)More proliferated cells were differentiated into neurons. Coronal sections were stained with anti-BrdU (red).
(G)Quantitative analysis of $BrdU^+GFP^+$ cells in GFP^+ in CP.
Data are the mean of five litters; error bars indicate SEM. Student's t-test, n.s., not significant; *P<0.05; **P<0.01. Scale bar, 50 μm.

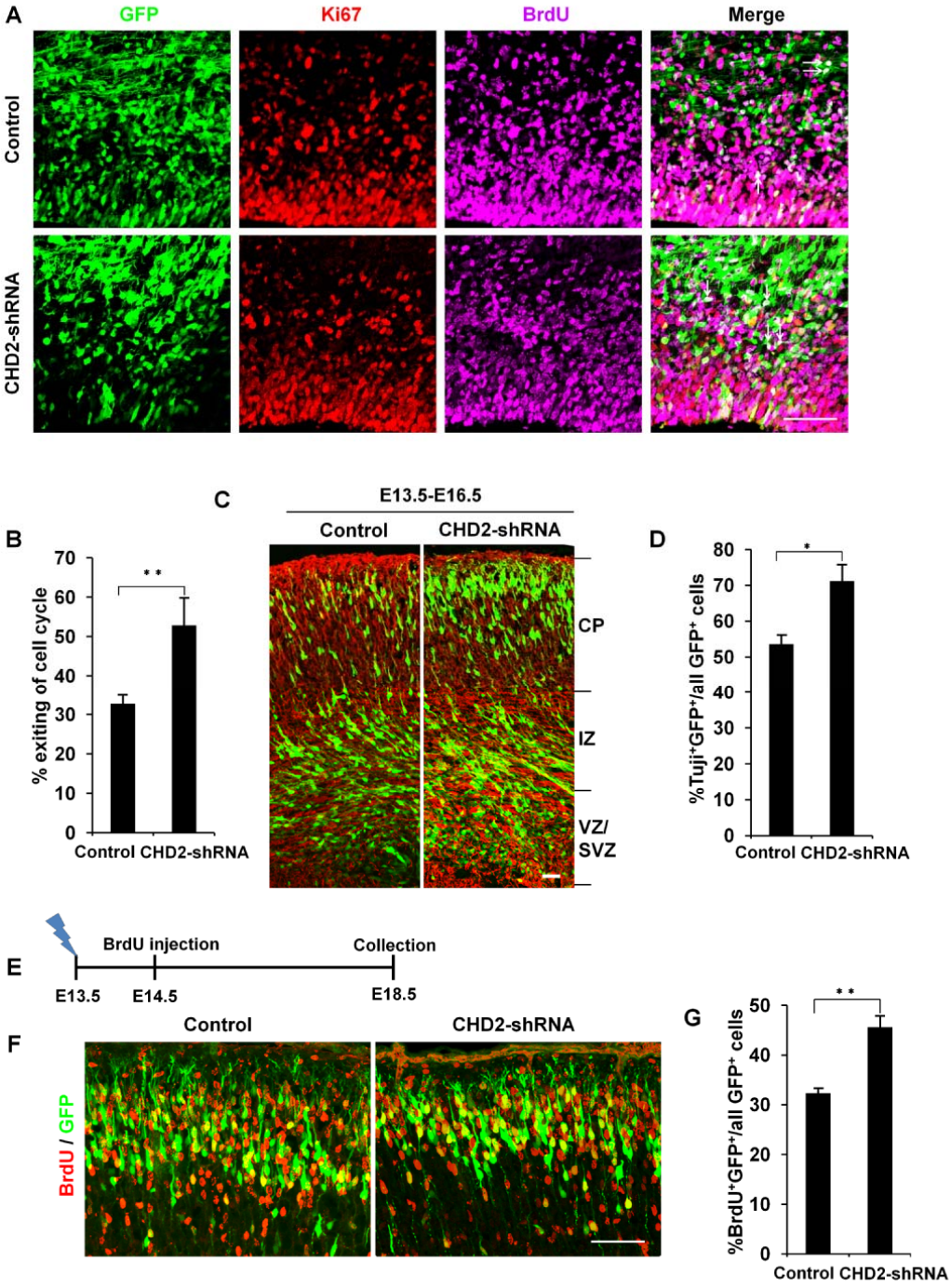

Shen et al., Figure 5

Figure 6. CHD2 regulates embryonic neurogenesis by promoting the expression of REST

(A): The expression of REST is down-regulated from E12 to E15. Quantitative PCR analysis of REST expression in cortex samples collected from different development stages. N=3 independent experiments.

(B): The expression of REST is down-regulated when CHD2 is silenced. Primary NSC cells infected with CHD2-shRNA or control lentivirus were used for the RT-PCR analysis. N=3 independent experiments.

(C): The distribution of GFP^+ cells in the REST-overexpressing cortex is similar to that in the CHD2-overexpressing cortex (Figure 2C). Data are the mean of five litters.

(D): The percentages of GFP^+ cells in the VZ/SVZ, IZ, and CP were quantified.

(E)Schematic illustration of the primer design for ChIP. Two pairs of primers were designed against sequences that were 1K and 2K upstream of the start codon of *REST*. One pair of primers was specifically binding the coding sequence of *REST*.

(F)The binding enrichment of *REST* is reduced when CHD2 is knocked down. Primay NSC was infected with control or CHD2 shRNA lentivirus and collected 3 days later for ChIP experiments. N=3 independent experiments.

(G)The binding enrichment of *REST* is increased when CHD2 is overexpressed. Primay NSC was infected with control or CHD2 overexpressing lentivirus and collected 3 days later for ChIP experiments. N=3 independent experiments.

(H): The western blotting analyses show that the fragments of CHD2 are expressed. Protein lysates were probed using antibodies against Flag. N=3 independent experiments.

(I): ChIP analysis shows that CHD2 regulates REST expression by binding to the genomic region of *REST.* The potential functional domain may be the chromatin-binding domain and DNA-binding domain. Primary NSC cells infected with Flag-tagged fragments of CHD2 were harvested and sonicated. The DNA fragments were quantified using real-time PCR with primers for the *REST* promoter and *REST* coding sequences. N=3 independent experiments.

Error bars indicate SEM. Student's t-test, n.s., not significant; *P<0.05; **P<0.01. Scale bar, 50 μm.

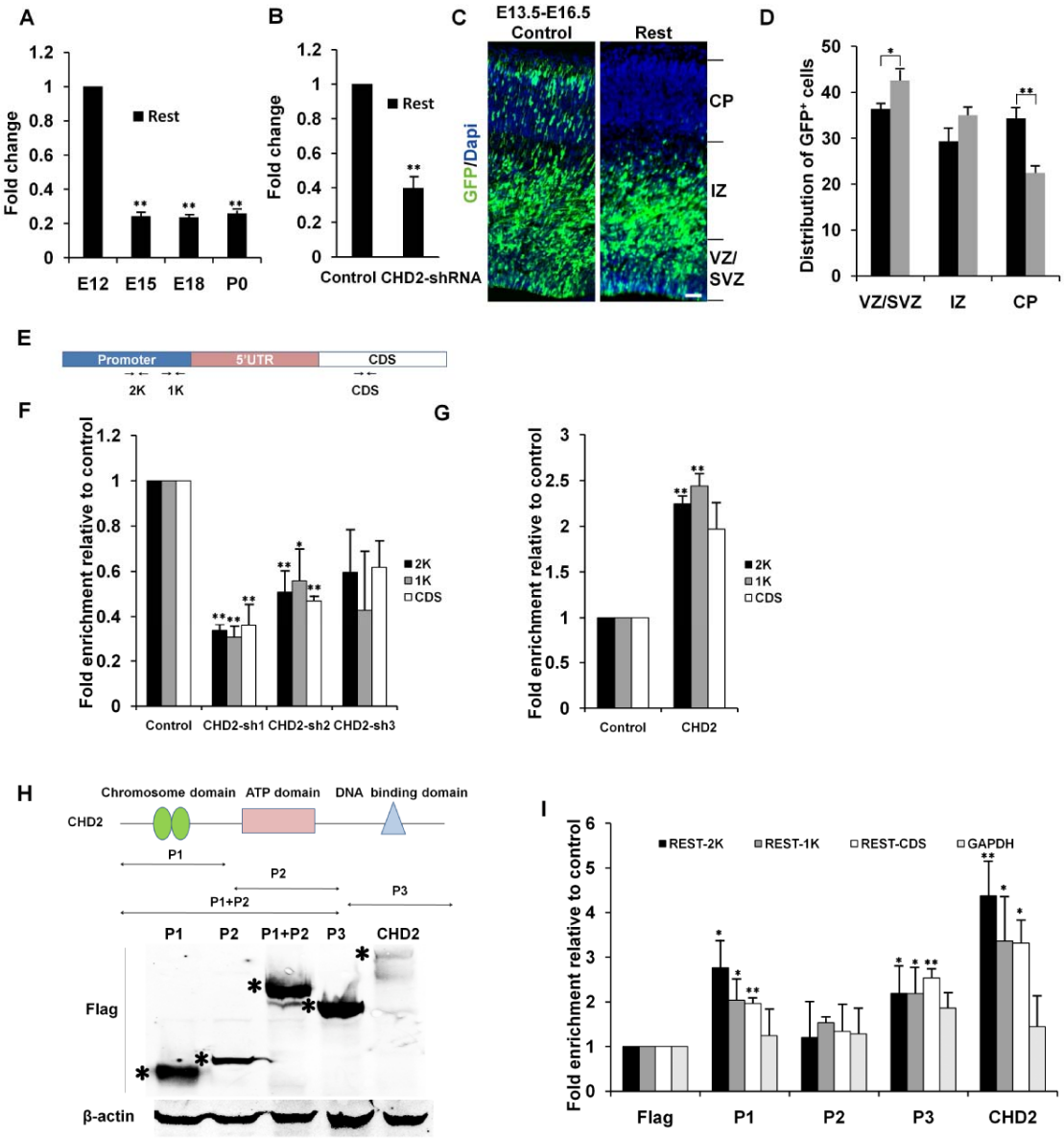

Shen et al, Figure 6

Figure 7. The defects caused by CHD2 depletion can be rescued via REST overexpression

(A): CHD2 or REST overexpression can rescue the cell positioning defects caused by CHD2 knockdown. The CHD2- or REST-overexpressing plasmid was electroporated with the CHD2-knockdown plasmid into the cortex at E13.5. The distribution of GFP^+ cells was investigated at E16.5.

(B): Quantification of GFP^+ cells in the VZ/SVZ, IZ, and CP.

(C): CHD2 or REST overexpression can rescue the amplification decrease of RGs caused by CHD2 knockdown. Coronal sections were stained using anti-Pax6 (red) and anti-BrdU (pink). The arrows indicate the $GFP^+/Pax6^+/BrdU^+$ cells.

(D): Percentage of $GFP^+Pax6^+BrdU^+$ cells divided by GFP^+Pax6^+ cells.

Data are the mean of five litters; error bars indicate SEM. Student's t-test, n.s., not significant; *P<0.05; **P<0.01. Scale bar, 50 μm.

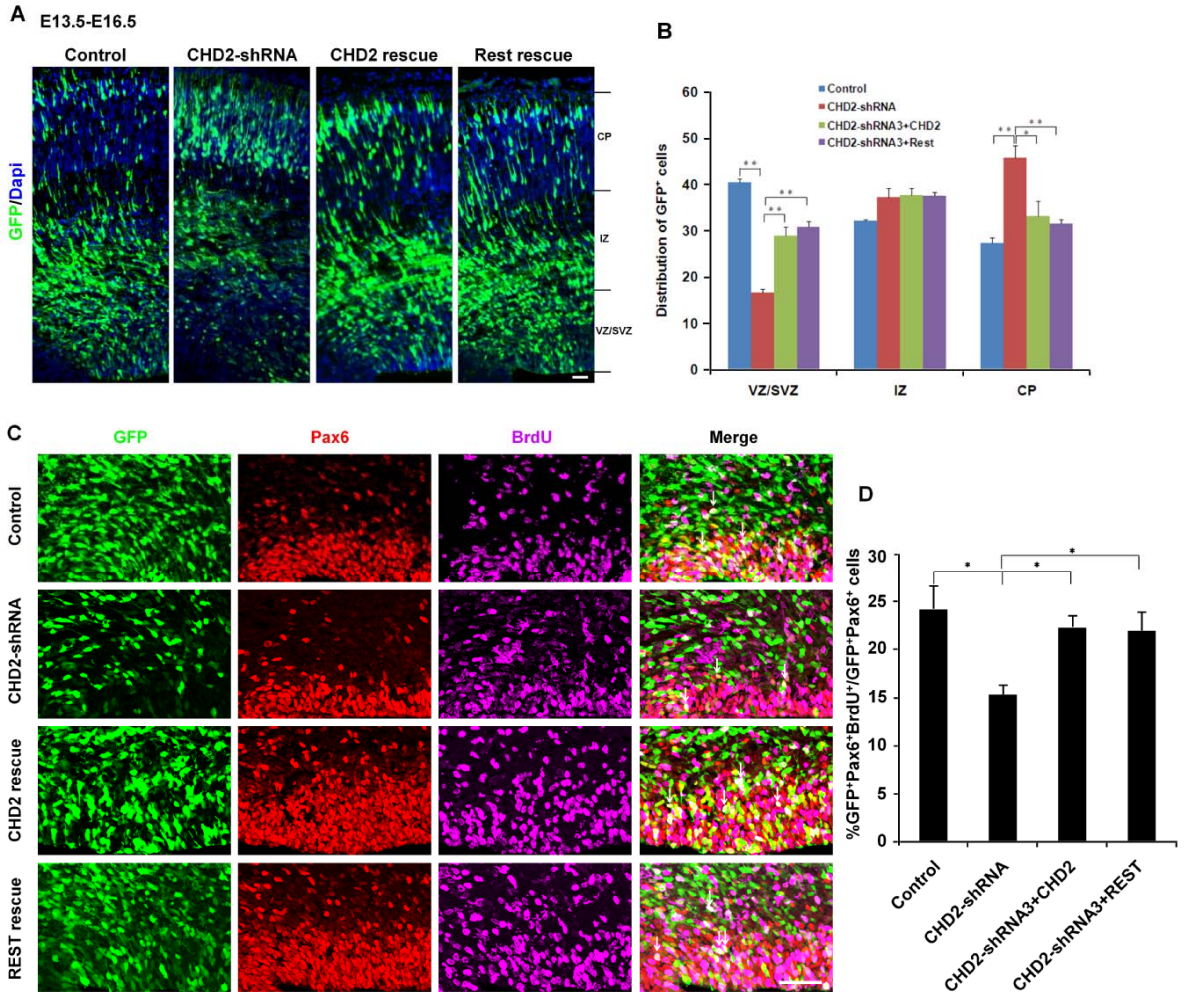

Shen et al., Figure 7